**Journal of Industrial Automation and Electrical Engineering**
Vol. 02, No. 01, June 2025, pp. 172~180
ISSN: 3089-1159


# Effect of Robot Speed on Cycle Time and Success Rate in Automated Cover Assembly and Screwing

**Raihan Nanda Adrianto[1], Risfendra[1]**
[1]Department of Electrical Engineering, Faculty of Engineering, Universitas Negeri Padang, Padang, Indonesia

**Article Info**

***Article history:***

Received April 11, 2025
Revised May 04, 2025
Accepted May 30, 2025

***Keywords:***

Industrial Robot
Assembly Process
screwing
Cycle time
Succes rate

**ABSTRACT**

This study investigates the effect of robot speed on cycle time and success rate in an automated cover assembly and screwing process. The experimental method was used to collect data by systematically varying the robot's movement speed and observing its impact on performance metrics. Experiments were conducted on a six axis Epson C4 industrial robot integrated with a Siemens S7 1200 programmable logic controller (PLC). Robot speed was adjusted across ten predefined levels from 6% to 33% of maximum velocity in 3% increments and for each level, three repeated trials were executed under controlled conditions. Results show that increasing speed from 6% to 33% reduces average cycle time from 908.6 s to 503.6 s for 4 product (227,1s–125,9s per product), a 44.6% improvement in efficiency. The relationship between speed and success rate is nonlinear: moderate speeds (27%–30%) yield an optimal success rate of 93.75% with cycle times of 517 s–533 s for 4 product (129s–133s per product), whereas both lower and maximum speeds decrease reliability due to vacuum pickup misalignment and screw retrieval inconsistencies. These findings underscore the need to balance speed and precision to optimize both efficiency and reliability in robotic assembly systems

***Corresponding Author:***

Raihan Nanda Adrianto
Department of Electrical Engineering, Faculty of Engineering, Universitas Negeri Padang
Kampus UNP Pusat, Jl. Prof. Hamka, Air Tawar, Padang 25131, Indonesia
Email: raihanadrianto14@gmail.com

## 1. INTRODUCTION

In recent years, industrial automation has played a critical role in improving the efficiency, precision, and consistency of assembly processes [1]. Robotic systems, particularly multi-axis articulated arms, are now widely implemented in automated assembly lines to perform complex tasks such as material handling, positioning, fastening, and inspection [2]. Among these, automated screwing and cover assembly are common tasks in electronics manufacturing, where accuracy and timing are essential [3]. According to the International Federation of Robotics, over 4 million industrial robots are currently in operation globally, underlining the growing reliance on robotic systems in manufacturing [4]. Despite this widespread adoption, one of the key factors that remains challenging to optimize is the robot's operational speed. The selection of appropriate speed settings is crucial, as it directly influences the cycle time and productivity of the system. If the robot operates too fast, it may result in positioning inaccuracies, increased vibration, or missed fastening points and decrease success rate [5], [6]. Conversely, lower speeds can reduce output efficiency and extend the production cycle

unnecessarily. Thus, understanding the relationship between robot speed and cycle time is vital for developing efficient and reliable automated systems [7].

Cycle time, defined as the total time required to complete one full unit of a product through all required operations in a production system, is a key metric used to assess operational efficiency [8]. An inefficient cycle time can hinder production goals and reduce the success rate, which refers to the proportion of assemblies completed correctly without errors or interruptions[9], while an optimized cycle time contributes significantly to higher throughput and better system utilization. To address this, Several studies have investigated trajectory and motion-planning algorithms to shorten cycle time [10]. However, most existing work treats assembly and fastening separately, without assessing their combined effect on overall timing Recent efforts have also explored cycle time optimization through energy-efficient robotic motion [11],[12], and multi-robot collaboration [13]. Nevertheless, the specific impact of speed variation on cycle time in integrated cover-assembly and screwing operations remains unquantified.

Furthermore, this system integrates a Programmable Logic Controller (PLC) to coordinate and manage communication between the robot and peripheral devices. The PLC ensures real-time control of inputs and outputs, synchronization of operations, and safety monitoring, thereby enhancing the reliability and flexibility of the assembly process [14]. The integration of the PLC with the six-axis robot enables precise timing control, thereby optimizing cycle time and enhancing overall system performance [15].

This paper aims to examine how variations in robot speed affect the cycle time in an integrated system designed for automatic cover assembly and screwing. The experiment involves a 6-axis industrial robot performing sequential pick-and-place and screw fastening operations on an ESP32 cover unit. The system is equipped with an HMI interface, tool changer, tool gripper, tool screwdriver, automatic screwfeeder, and conveyor. Data were gathered at multiple robot speed settings to analyze changes in cycle time and success rate, aiming to determine the most effective operating parameters.

## 2. METHOD

This study employs an experimental method to examine the effect of robot speed on cycle time and success rate in an automated cover assembly and screwing system. The experiments were conducted on a 6-axis Epson C4 industrial robot integrated with a Siemens S7-1200 programmable logic controller (PLC), supported by various input-output (I/O) devices such as sensors and actuators.

Robot speed was systematically varied across ten predefined levels, ranging from 6% to 33% of the maximum velocity in 3% increments. At each speed level, three repeated trials were conducted under controlled conditions to ensure data consistency[16]. In each trial, the robot executed a standardized sequence of operations picking, placing, and screwing for the assembly of four products. Cycle time for each trial was recorded directly from the Human-Machine Interface (HMI), which displayed the total duration required to complete the full assembly cycle. A block diagram presented in Figure 1 illustrates the system architecture and signal flow, providing a visual overview of data communication throughout the assembly process.

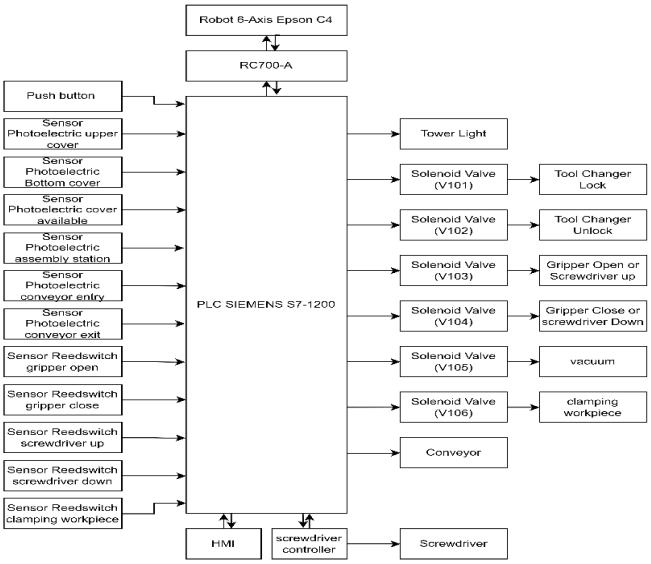


Figure 1. Block diagram systems

Based on the block diagram presented in Figure 1, the automated assembly system comprises several key components that are seamlessly integrated to support a fully coordinated and autonomous operation. The 6-axis Epson C4 robot is controlled via the RC700-A controller and receives instructions from the Siemens S7-1200 PLC, which functions as the central processing unit. The PLC processes input signals from various sensors, such as photoelectric sensors, reed switches, and push buttons. These signals are used to actuate various devices including solenoid valves, conveyors, tower lights, and the robot's end-effector tools. Additionally, the system is equipped with a Human-Machine Interface (HMI) allowing operators to monitor and interact with the system in real-time. This integration facilitates bidirectional communication among components, ensuring synchronized and safe execution of each assembly cycle. The coordinated workflow serves as the foundation for evaluating the influence of robot movement speed on the overall cycle time performance.

Figure 2 presents a sketch of the working principle for the automated assembly system. The diagram illustrates the interaction between the 6-axis robot, tool gripper, tool screwdriver, tool changer, upper cover, bottom cover, pallet 2x2 ESP32, automatic screwfeeder, assembly station, and conveyor, highlighting the sequential flow of components and tools throughout the assembly process.

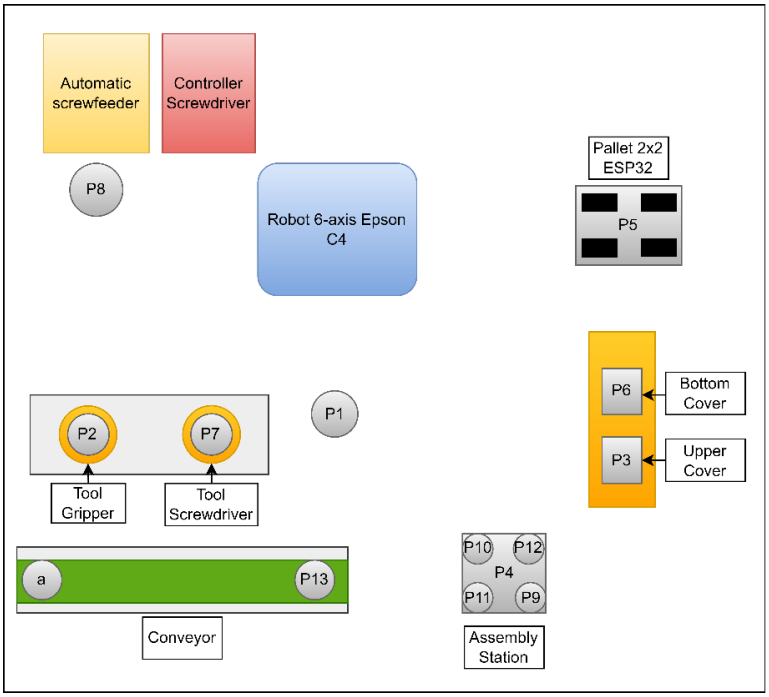


Figure 2. Sketch of the working principle

Based on Figure 2, the system sequence initiates at the home position (P1). The robot first moves to the tool gripper station (P2) utilizing the tool changer system. Subsequently, the robot retrieves the upper cover (P3), which is placed at the assembly station (P4), and then proceeds to pick up the ESP32 at position (P5), returning it to the assembly station. The robot then collects the bottom cover (P8) and places it at the assembly station as well. Following this, the robot returns the tool gripper and switches to the tool screwdriver (P7). With the tool screwdriver attached, the robot acquires a screw from the automatic screw feeder (P8) and moves to screw position 1 (P9) located at the assembly station. This process is repeated: the robot returns to the automatic screw feeder to obtain another screw and proceeds to screw position 2 (P10). This sequence continues iteratively for screw positions 3 (P11) and screw positions 4 (P12). After completing the screwing process, the robot returns the tool screwdriver and reattaches the tool gripper. The tool gripper then picks up the product from the assembly station and places it onto the conveyor entry (P13). The conveyor is then activated, transporting the product to the conveyor exit sensor (a). While waiting for the product to reach the conveyor exit, the robot returns to the home position. Once the product has arrived at the conveyor exit and has been collected by the operator, the robot repeats the entire assembly cycle up to four times. After assembling four products, the robot returns the tool gripper and moves to the home position. The detailed work sequence, including each step of the automated cover assembly and screwing process is comprehensively illustrated in Figure 3.

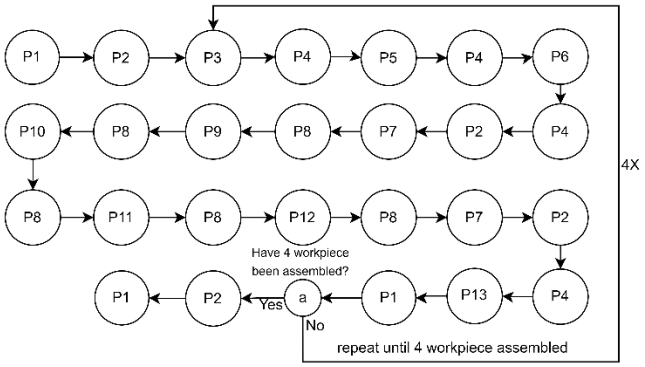


Figure 3. work Sequence system

To further clarify the workflow, a flowchart is provided to illustrate the process systematically and structurally in figure 4. This diagram helps visualize the sequence of instructions and stages involved in the automated cover assembly and screwing system, enabling a clearer understanding of the overall process flow.

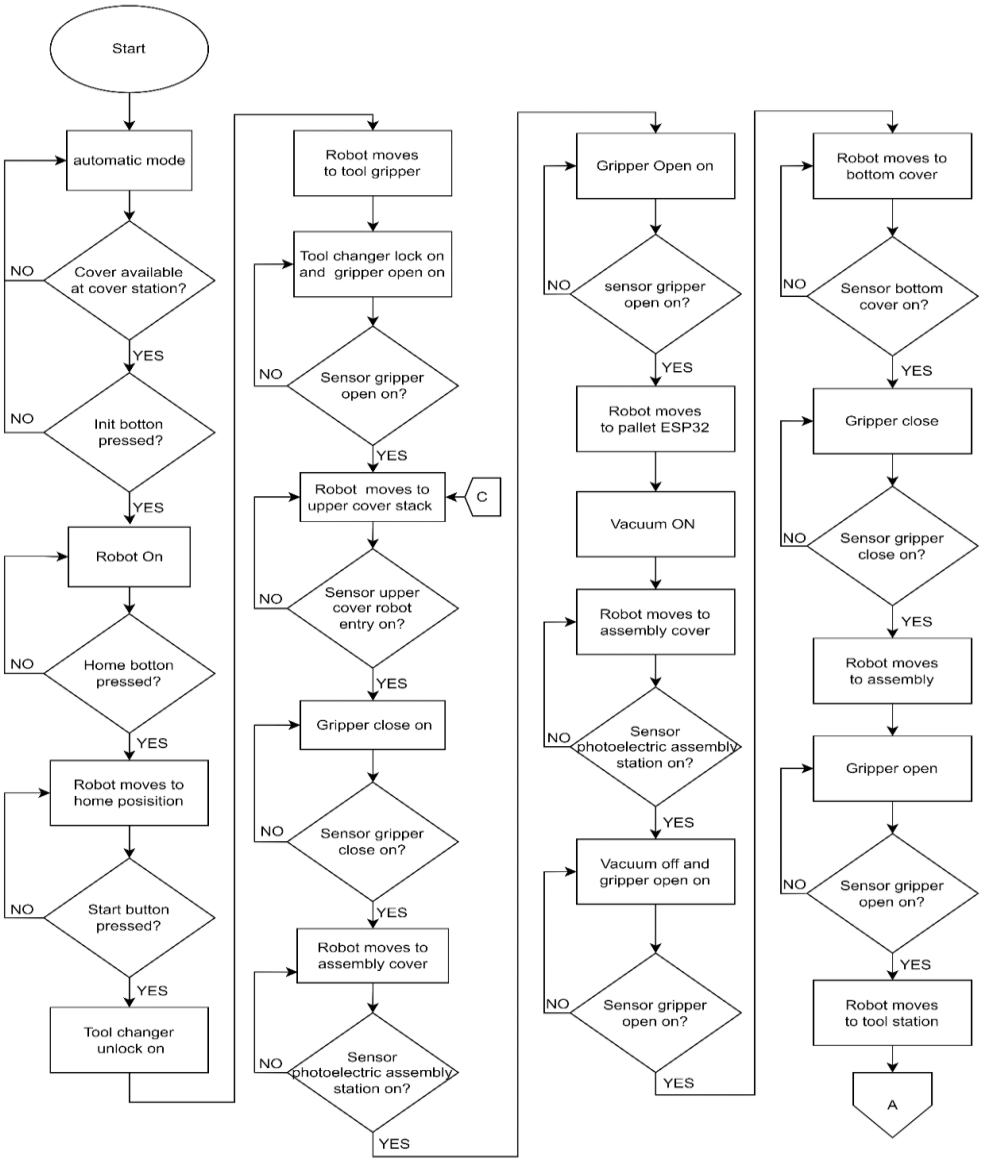


Figure 4. Flowchart system

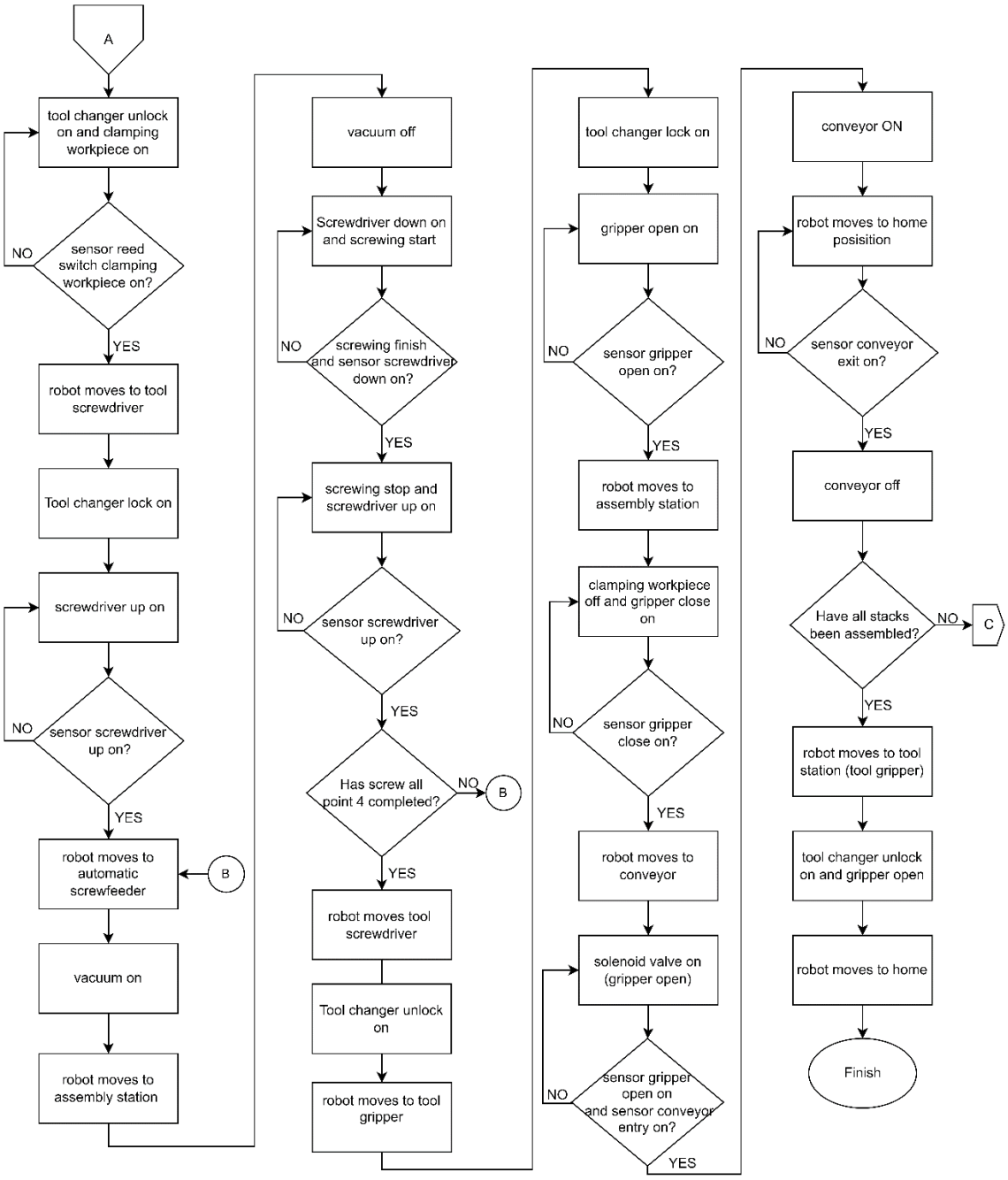


Figure 5. (Continued) Flowchart system

The automated cover assembly and screwing system, shown in the flowchart in Figure 4 and figure 5, begins with operator verification of the upper and bottom covers at their stations, supported by visual inspection and status indicators on the Human-Machine Interface (HMI). After confirming component availability, the operator powers on and initializes the robot by pressing the init button, moves it to the home position via the home button, and then starts the operation by pressing the start button to begin the automated process. Once started, the robot initiates a tool change to attach the appropriate tool gripper and verified by corresponding sensors and solenoid valves. It then sequentially retrieves the upper cover, the ESP32 unit, and the bottom cover, placing each component onto the assembly station. A photoelectric sensor detects the presence of a cover at the assembly station before the robot proceeds with placement, ensuring the station is ready for the next step.

After completing the placement steps, the robot returns to the tool station to exchange the gripper for the screwdriver tool. This tool change is carried out using a tool changer mechanism and verified by corresponding sensors and solenoid valves. Once the screwdriver tool is secured, the robot performs the

screwing operation on all four designated screw points using a vacuum-based screwing mechanism. This step is critical to securing the assembled components, with each movement executed along a predefined motion path and speed configured in the robot controller. Following the screwing process, the robot switches back to the tool gripper, picks up the fully assembled product, and transfers it to the conveyor. While the conveyor moves the product to the output area, the robot returns to its home position and waits for the exit sensor to confirm successful product transfer. This process repeats until all four products in the batch are completed. Upon finishing the fourth cycle, the robot places the gripper back into its holder and returns to the home position, indicating the end of the operation sequence.

## 3. RESULTS AND DISCUSSION

This section presents the results obtained from the experimental testing of the automated cover assembly and screwing system. A top-view image of the integrated work cell is shown in Figure 6, to provide a visual overview of the physical arrangement of system components, including the 6-axis robot, tool changer, tool gripper, tool screwdriver, upper cover and bottom cover, screw feeder, and conveyor. This real system layout corresponds to the schematic sketch previously illustrated in Figure 2, demonstrating how the conceptual design was implemented in the physical setup. The spatial configuration was designed to optimize the task sequence and minimize the robot's travel distance, which directly affects overall cycle time performance. The Human-Machine Interface (HMI), as shown in Figure 7, is equipped with a real-time cycle time display, enabling operators to monitor the total duration of each assembly cycle. This measurement served as the primary reference for evaluating the impact of robot speed variations on system performance

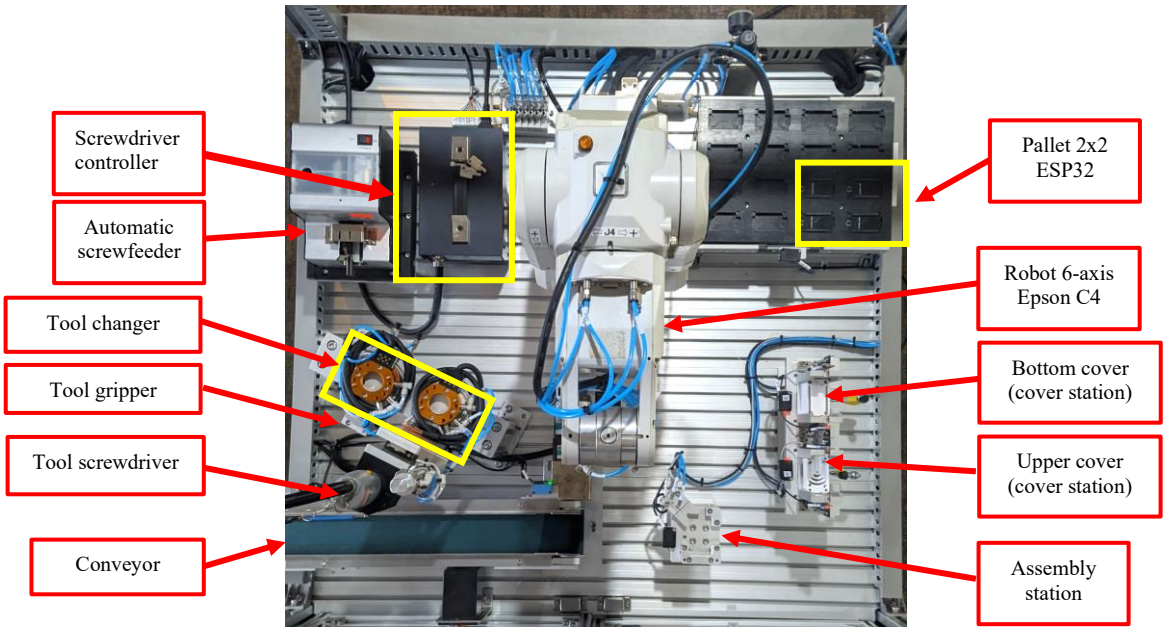


Figure 6. Top view automated cover assembly and screwing

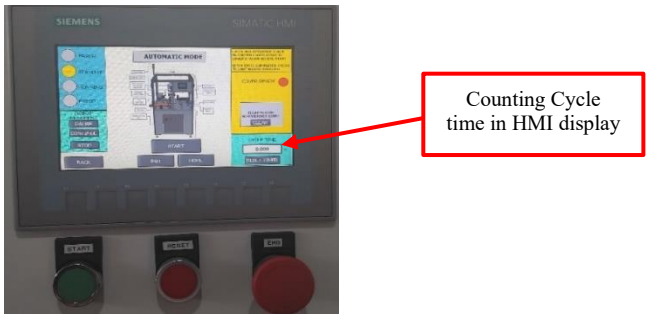


Figure 7. shows the Human-Machine Interface (HMI) with a digital cycle time display, mounted above three physical pushbuttons

Table 1 presents the experimental results showing the average success rate and cycle time at each robot speed level. Three trials were conducted at every speed setting from 3% to 33% to ensure statistical robustness, account for operational variability, and validate repeatability.

Table 1. cycle time and success rate at various robot speeds in automated cover assembly and screwing

| Speed robot | Average cycle time (s) | Average success rate (%) |
|---|---|---|
| 6% | 908.6 | 97.91 |
| 9% | 767.0 | 95.83 |
| 12% | 685.0 | 93.75 |
| 15% | 635.0 | 93.75 |
| 18% | 599.7 | 93.75 |
| 21% | 572.9 | 87.5 |
| 24% | 549.2 | 77.08 |
| 27% | 533.0 | 93.75 |
| 30% | 517.7 | 93.75 |
| 33% | 503.6 | 91.67 |

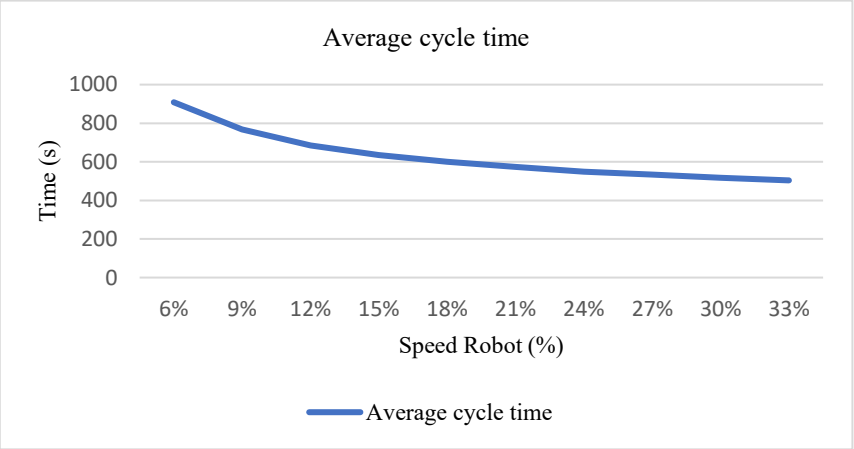


Figure 8. Average cycle time

Based on the experimental results in Table 1 and the graph shown in Figure 8, a clear inverse correlation between robot speed and cycle time is observed. As robot speed increased from 6% to 33%, the average cycle time decreased significantly from 908.6 seconds to 503.6 second (227.1 s to 125.9 s per product). representing a total reduction of approximately 44.6%. This trend is expected, as higher movement speeds shorten the duration of each task in the assembly and screwing processes. Notably, the largest time reduction occurred within the lower speed range (6–12%), while the time savings became marginal beyond 27% speed, indicating diminishing returns in terms of efficiency gains. Despite these improvements in cycle time, higher speeds must be carefully balanced with precision requirements, as excessive speed may introduce performance instability, as observed in the success rate data.

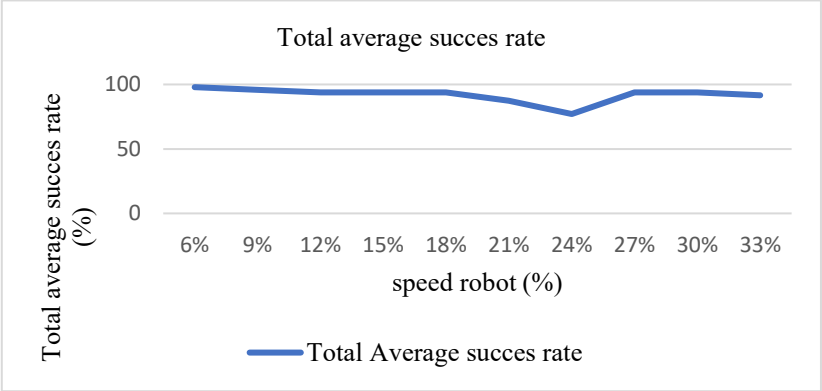


Figure 9. Total Average success rate

As illustrated in Figure 9, the success rate exhibits a nonlinear relationship with robot speed, contrasting the inverse correlation observed in cycle time. At 24% speed, the success rate drops sharply to 77.08%, with one trial recording 62.5% due to incomplete assemblies (Table 2). As shown in Figure 10, the assembly station displays only the upper and bottom covers secured, while the ESP32 module remains missing direct consequence of positional misalignment during vacuum pickup.

Table 2. cycle time and success rate at 70% robot speeds in automated cover assembly and screwing

| Speed | Attemp Number | Succes rate product 1 | Succes rate product 2 | Succes rate product 3 | Succes rate product 4 | Average all product succes rate (%) | Cycle time (s) |
|---|---|---|---|---|---|---|---|
| 70% | 1 | 100 | 100 | 100 | 50 | 87.5 | 549.9 |
| | 2 | 75 | 75 | 75 | 100 | 81.25 | 548.4 |
| | 3 | 75 | 100 | 75 | 0 | 62.5 | 549.3 |
| | | | | | **Total average** | **77.08** | **549.2** |

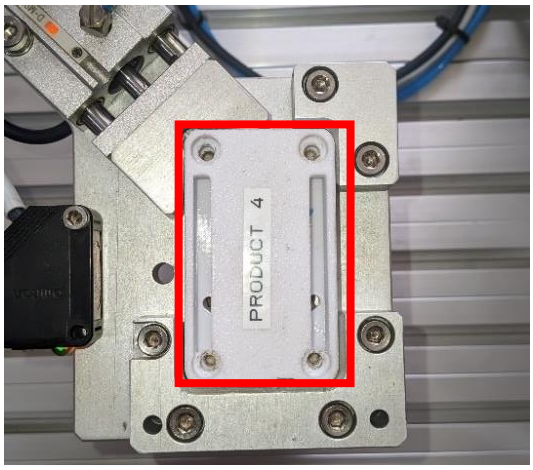


Figure 10. Assembly failure due to missing ESP32 module within the cover at the assembly station

At speeds of 27%–30%, the system achieved a stable success rate of 93.75%, with total cycle times of 517 s–533 s for four products (129 s–133 s per product), as slower acceleration ensured precise alignment of the vacuum nozzle during component retrieval. However, at 33% speed, minor inconsistencies re-emerged (91.67% success rate), primarily due to failed screw retrieval from the automatic screw feeder during high-speed operation. However, rapid motion occasionally caused misalignment between the nozzle and screw channel, leading to partial or missed pickups. Despite this, Figure 11, demonstrates a fully assembled product from the third trial at 33% speed, achieving 100% success rate in one attempt, where optimal alignment was temporarily restored.

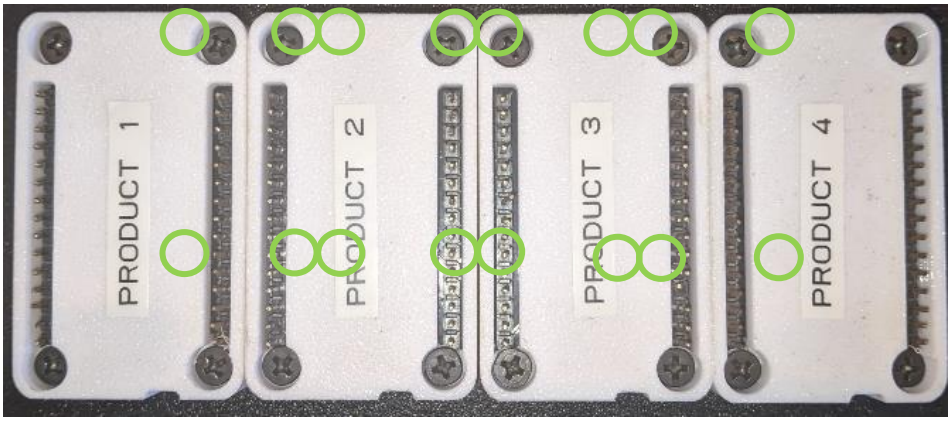


Figure 5. fully assembled product from the third trial at 33% speed

## 4. CONCLUSION

The experimental results demonstrate that increasing the robot speed from 3% to 33% significantly reduces the total cycle time from 908.6 s to 503.6 s (227.1 s to 125.9 s per product). However, the relationship between speed and assembly success rate is nonlinear. While moderate speeds maintain high reliability, a sharp decline in success rate is observed at 24% speed, primarily due to misalignment during screw vacuum pickup. At the maximum speed of 33%, minor inconsistencies reoccur as a result of failed screw retrievals. The optimal operational range is identified at speeds of 27%–30%, where the system achieves a stable and high success rate of 93.75%, with minimized cycle times of 517 s–533 s to 4 products assembled (129 s–133 s per product). These findings underscore the necessity of balancing operational efficiency and reliability in automated robotic assembly systems.

## ACKNOWLEDGEMENTS

The author expresses sincere gratitude to the Teaching Factory of Industrial Robotics and Automation at Padang State University, as well as to PT UNPMES Inovasi Indonesia, for the valuable opportunity and support in facilitating the on-site research.

## REFERENCES

[1] H. T. Anaam K I and P. A. Y. W. Pranata R Y, Abdillah h, "Pengaruh Trend Otomasi Dalam Dunia Manufaktur dan Industri," *Vocat. Educ. Natl. Semin.*, vol. 1, no. 1, pp. 46–50, 2022.

[2] L. Liu, "Application Status and Development Trend of Industrial Robots in China," no. Ieesasm, pp. 249–255, 2020, doi: 10.25236/ieesasm.2020.048.

[3] Ş. Çiğdem, I. Meidute-Kavaliauskiene, and B. Yıldız, "Industry 4.0 and Industrial Robots: A Study from the Perspective of Manufacturing Company Employees," *Logistics*, vol. 7, no. 1, 2023.

[4] A. Minsandi *et al.*, "Design and Implementation of Robot Abu Robocon Using Joystik Wireless Based on Extrasenory Percepsion," *J. Ind. Autom. Electr. Eng.*, vol. 01, no. 01, pp. 39–45, 2024

[5] M. P. Cooper, C. A. Griffiths, K. T. Andrzejewski, and C. Giannetti, "Motion optimisation for improved cycle time and reduced vibration in robotic assembly of electronic components," *AIMS Electron. Electr. Eng.*, vol. 3, no. 3, pp. 274–289, 2019, doi: 10.3934/ElectrEng.2019.3.274.

[6] M. Morozov *et al.*, "Assessing the accuracy of industrial robots through metrology for the enhancement of automated non-destructive testing," *IEEE Int. Conf. Multisens. Fusion Integr. Intell. Syst.*, vol. 0, no. 0, pp. 335–340, 2016, doi: 10.1109/MFI.2016.7849510.

[7] V. Bucinskas *et al.*, "Improving Industrial Robot Positioning Accuracy to the Microscale Using Machine Learning Method," *Machines*, vol. 10, no. 10, 2022, doi: 10.3390/machines10100940.

[8] A. Abustan and R. Syam, "Omniwheels Dengan Manipulator Untuk Robot Penjinak Bom," *mekanikal*, vol. 6, no. 1, pp. 557–564, 2015.

[9] J. Marvel and J. Falco, "Best Practices and Performance Metrics Using Force Control for Robotic Assembly," 2012, [Online]. Available: http://nvlpubs.nist.gov/nistpubs/ir/2012/NIST.IR.7901.pdf

[10] H. K. Banga, P. Kalra, R. Kumar, S. Singh, and C. I. Pruncu, "Optimization of the cycle time of robotics resistance spot welding for automotive applications," *J. Adv. Manuf. Process.*, vol. 3, no. 3, pp. 1–11, 2021, doi: 10.1002/amp2.10084.

[11] Risfendra, Yoga Maulana Putra, H. Setyawan, and M. Yuhendri, "Development of Outseal PLC-Based HMI as Learning Training Kits for Programmed Control Systems Subject in Vocational Schools," in *5th Vocational Education International Conference*, 2023, pp. 506–511.

[12] S. Gürel, H. Gultekin, and N. Emiroglu, "Scheduling a dual gripper material handling robot with energy considerations," *J. Manuf. Syst.*, vol. 67, pp. 265–280, 2023.

[13] P. Huang, R. Liu, C. Liu, and J. Li, "APEX-MR: Multi-Robot Asynchronous Planning and Execution for Cooperative Assembly," vol. 1, 2025, [Online]. Available: http://arxiv.org/abs/2503.15836

[14] X. Sun and C. Peng, "Novel Motion Control System for Industrial Robot Arms Enhanced by Innovative Method and PLC Integration," in *2024 IEEE 33rd International Symposium on Industrial Electronics (ISIE)*, 2024, pp. 1–6. doi: 10.1109/ISIE54533.2024.10595769.

[15] D. Spensieri, E. Åblad, R. Bohlin, J. S. Carlson, and R. Söderberg, "Modeling and optimization of implementation aspects in industrial robot coordination," *Robot. Comput. Integr. Manuf.*, vol. 69, p. 102097, 2021, doi: 10.1016/J.RCIM.2020.102097.

[16] Y. Chuangui, M. Liang, L. Xingbao, X. Yangqiu, Q. Teng, and L. Han, "Uncertainty evaluation of measurement of orientation repeatability for industrial robots," *Ind. Robot Int. J. Robot. Res. Appl.*, vol. 47, no. 2, pp. 207–217, Jan. 2020, doi: 10.1108/IR-07-2019-0145.